

Accurate Adiabatic Connection Curve Beyond the Physical Interaction Strength

R. J. Magyar

Department of Physics, Rutgers University, 136 Frelinghuysen Road, Piscataway, NJ 08854-8019

W. Terilla

Department of Chemistry, Rutgers University, 610 Taylor Road, Piscataway, NJ 08854-8019

K. Burke

*Department of Chemistry and Chemical Biology,
Rutgers University, 610 Taylor Road, Piscataway, NJ 08854-8019*

(Dated: November 15, 2018)

The adiabatic connection curve of density functional theory (DFT) is accurately calculated beyond the physical interaction strength for Hooke's atom, two interacting electrons in a harmonic well potential. Extrapolation of the accurate curve to the infinite coupling limit agrees well with the strictly correlated electron (SCE) hypothesis but the approach to this limit is more complex. The interaction strength interpolation is shown to be a good, but not perfect, fit to the adiabatic curve. Arguments about the locality of functionals and convexity of the adiabatic connection curve are examined in this regime.

PACS numbers: 31.15.Ew, 71.15.Mb, 71.10.-w, 73.21.La

I. INTRODUCTION

Density functional theory (DFT) is a popular computational method in solid state physics and quantum chemistry since it is both simple and reliable [1–3]. Because of its wide range of applications and its ability to handle large systems, there is considerable interest in DFT and improving its accuracy. In DFT, the only part of the total energy to approximate is the exchange-correlation energy functional, $E_{xc}[n]$. A formal and general expression for the exchange-correlation energy is according to the adiabatic connection [4],

$$E_{xc}[n] = \int_0^1 d\lambda U_{xc}[n](\lambda). \quad (1)$$

where $U_{xc}[n](\lambda)$ is the exchange-correlation potential energy of a density, n , at coupling constant, λ . Analysis of the integrand, $U_{xc}[n](\lambda)$, leads to many exact relationships that the exact exchange-correlation energy satisfies and approximate functionals should satisfy. For example, Görling and Levy obtained a perturbation series expression for the exchange-correlation energy [5] by expanding about the weak interaction limit. Another fruitful result is the understanding of why hybrid functionals like PBE0 [6] and B3LYP [7] perform so well [8–10].

Because the exchange-correlation energy is the area under the adiabatic connection curve between $\lambda = 0$ to 1, the most interest in $U_{xc}(\lambda)$ has been confined to this domain. However, there is no fundamental reason to restrict study to this domain. In fact, certain exact properties of the adiabatic connection curve outside this domain have

been used to better approximate the curve [11]. One example is the consideration of the strong interaction limit, $\lambda \rightarrow \infty$. A model for this strongly interacting limit is the strictly correlated electron (SCE) hypothesis [12, 13] which states that, because of the strong Coulomb repulsion, the individual electrons distribute themselves as far apart as possible but are constrained to yield a given density. Finding one electron uniquely pins the others into position. Among other predictions, this SCE model says that U_{xc} can also be expanded about the strong interaction strength limit ($\lambda \rightarrow \infty$). Information from this infinite limit combined with the Görling-Levy expansion about $\lambda = 0$ leads to the suggestion of the interaction strength interpolation (ISI) for the entire curve. Exchange-correlation energies from the ISI are considerably more accurate than those using only the first two terms in the perturbation series [14].

Another reason to consider large coupling strengths is that approximate exchange-correlation energy functionals for this limit might be more accurate [15]. It has long been known that standard approximate density functionals, such as the local density approximation (LDA) or the PBE generalized gradient approximation (GGA), are better for exchange-correlation together than they are for exchange alone. This is due to a cancellation of errors between approximations to the exchange and correlation energy [10, 16]. If this cancellation between exchange and correlation grows with larger coupling constants, approximate density functionals in this regime will be more accurate.

The present work is a detailed study of some of these suggestions. We employ a procedure developed for the range $\lambda = 0$ to 1 [17] and extend the simulated adiabatic

connection curve to larger coupling constants. At some point along the adiabatic connection curve, the simulating scaling method is expected to break down. Nevertheless, the curve can be extrapolated from there to the infinite coupling limit. This analysis yields interesting new information about the strong interaction limit.

We work with Hooke's atom because it remains bound no matter how strongly the electrons interact. Hooke's atom is the unpolarized two electron system described by the Hamiltonian [?] ,

$$\hat{H} = -\frac{1}{2}(\nabla_1^2 + \nabla_2^2) + \frac{k}{2}(\mathbf{r}_1^2 + \mathbf{r}_2^2) + \frac{1}{|\mathbf{r}_1 - \mathbf{r}_2|}, \quad (2)$$

where k is the harmonic force constant, \mathbf{r}_1 and \mathbf{r}_2 are the position operators for each electron, and ∇_1^2 and ∇_2^2 are the Laplacian operators for each. Throughout, we use atomic units ($e^2 = \hbar = m_e = 1$) so that all energies are in Hartrees and all lengths in Bohr radii. This is not just an exactly solvable model with Coulomb interactions but also an important *physical system*. For example, many authors have used this system to model quantum dots [19, 20].

Although we could have performed calculations for the Hooke's atom at various harmonic well strengths, we will focus on $k = 1/4$. For this spring constant, the Hooke's atom happens to admit an analytic solution [21]. Furthermore, for this k value, the correlation energy is comparable to that of the Helium atom.

The simulated curves indicate that the SCE predictions for $U_{xc}(\infty)$ are correct. Next, assuming the validity of the SCE hypothesis, we generate a highly accurate simulation of the entire curve. This allows us to calculate higher derivatives of $U_{xc}(\lambda)$ around key points: $\lambda = 0, 1$, and ∞ . This information should be useful for the testing and improvement of existing functionals. We also compare the interaction strength interpolation (ISI) with the accurate simulated result.

II. ADIABATIC CONNECTION THEORY

Three theoretical elements are vital to the content of this paper. These are the adiabatic connection curve, the strong coupling limit, and the relationship between scale factor and coupling constant.

First, we review the adiabatic connection formalism. The integrand of Eq. (1) is

$$U_{xc}[n](\lambda) = \langle \Psi_n^{min,\lambda} | \hat{V}_{ee} | \Psi_n^{min,\lambda} \rangle - U[n], \quad (3)$$

where $U[n]$ is the Hartree energy, \hat{V}_{ee} is the electron-electron Coulomb interaction, and $\Psi_n^{min,\lambda}$ is the wavefunction that minimizes $\langle \Psi_n^{min,\lambda} | \hat{T} + \lambda \hat{V}_{ee} | \Psi_n^{min,\lambda} \rangle$ and yields the density $n(\mathbf{r})$. The functional, $U_{xc}[n](\lambda)$, as a function of λ makes up the adiabatic connection curve. At $\lambda = 0$, Eq. 3 is just E_x , the exchange energy evaluated at a given density. Later for convenience, we will subtract this contribution and write $U_C(\lambda) = U_{xc}(\lambda) - E_x$.

At small λ , one may write the Görling-Levy perturbation series [22]:

$$U_{xc}[n](\lambda) = E_x[n] + 2E_C^{GL2}[n]\lambda + \mathcal{O}(\lambda^2), \quad \lambda \rightarrow 0 \quad (4)$$

where E_x is the exchange energy, and $E_C^{GL2}[n]$ is the first order contribution to the correlation energy. To get the exchange-correlation energy from Eq. (4), we need to integrate from $\lambda = 0$ to 1. Unfortunately, there is no guarantee that the higher order terms will be negligible and that the series will converge [14].

Other exact properties of U_{xc} might be useful to help understand this curve. An interesting limit is when $\lambda \rightarrow \infty$. This leads us to the second theoretical point, the strong coupling limit. This limit corresponds to strongly interacting electrons which still yield the physical density. In this limit, the integrand is finite [13]. We can expand $U_{xc}(\lambda)$ about the infinite limit:

$$U_{xc}[n](\lambda) = U_{xc}[n](\infty) + U'_{xc}[n](\infty)/\sqrt{\lambda} + \mathcal{O}(1/\lambda), \quad \lambda \rightarrow \infty \quad (5)$$

where $U_{xc}[n](\infty)$ and $U'_{xc}[n](\infty)$ are the zeroth and first terms in the expansion. It has been suggested that the electrons behave in a strictly correlated manner at this limit [13]. The electrons still produce a given density distribution, but finding one electron determines the position of all the others. Information about this limit can be incorporated into an interpolation formula which reproduces both limits exactly and can be integrated analytically. An example is the Interaction Strength Interpolation (ISI) [14].

For spherically symmetric two-electron systems in three dimensions, the SCE model admits an exact solution for $U_{xc}(\infty)$ and provides one of two contributions to $U'_{xc}(\infty)$ [13]. One question asked in this paper is how large the missing contribution to $U'_{xc}(\infty)$ is. We have calculated the SCE limit and part of the first correction term for the Hooke's atom $k = 1/4$ according to the formulae given by Seidl in Ref. [13].

The final point, the relationship between coupling constant and scale factor, is important for the procedure we used to simulate the adiabatic connection curve. A density, $n(\mathbf{r})$, is scaled according to

$$n_\gamma(\mathbf{r}) = \gamma^3 n(\gamma\mathbf{r}), \quad 0 \leq \gamma < \infty. \quad (6)$$

with γ being the scale factor. The exchange-correlation energy at a coupling constant, λ , and density, $n(\mathbf{r})$, is simply related to the exchange-correlation energy at a scaled density [23, 24]:

$$E_{xc}^\lambda[n] = \lambda^2 E_{xc}[n_{1/\lambda}]. \quad (7)$$

The integrand in Eq. (1) is $U_{xc}(\lambda) = dE_{xc}^\lambda/d\lambda$. Under both coupling constant and scaling transformations, we can sometimes show how parts of the exact energy transform. For example,

$$E_x^\lambda[n] = \lambda E_x[n] \text{ or } E_x[n_\gamma] = \gamma E_x[n]. \quad (8)$$

We use this observation later to identify scale factors between two scaled densities.

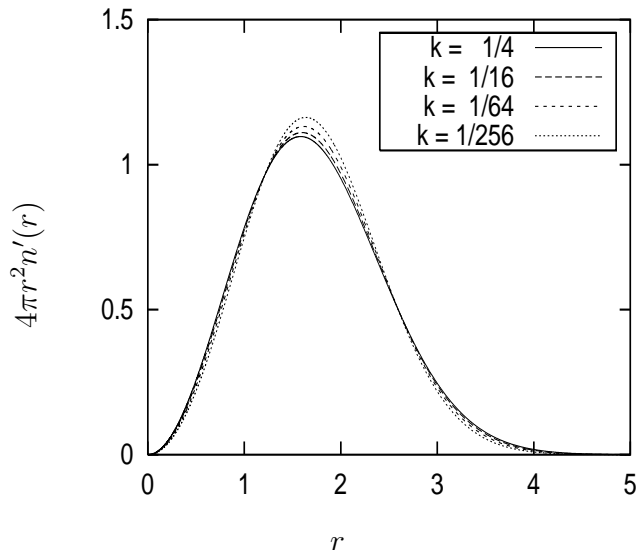


FIG. 1: Simulated scaling of the density. We start with Hooke’s atom at $k = 1/4$. Then, we solve at various other coupling constants and use the simulated scaling to return us as closely as possible to the $k = 1/4$ density.

III. SIMULATED SCALING METHOD

In order to generate highly accurate adiabatic connection plots, we use the procedure developed by Frydel, Terilla, and Burke [17]. To find the adiabatic connection curve, we need $E_{xc}^\lambda[n]$ for a set of λ ’s. For Hooke’s atom, we know the exact densities and the exact E_{xc} at different k values. Instead of changing λ , which is difficult, we use Eq. (7). A small change in the strength of external potential yields another density, qualitatively similar to the original density but on a different scale. If we can solve the system exactly at this different external potential strength, we have an approximation to the exchange-correlation energy with a scaled density. For densities that do not qualitatively change shape much, this scheme is highly accurate. To find $U_{xc}(\lambda)$, we differentiate Eq. (7) with this highly accurate approximation to the exact $E_{xc}[n_{1/\lambda}]$. Including a first order correction term increases the accuracy of this method:

$$E_c[n_\gamma] \approx E_c[n'] + \int d^3r v_c[n'](\mathbf{r})(n_\gamma(\mathbf{r}) - n'(\mathbf{r})) + \mathcal{O}(\delta n)^2, \quad (9)$$

TABLE I: Simulated scaling k and λ equivalences using the E_x scaling rule, Eq. (10), to determine λ .

k	λ	k	λ
1/4	1.000	1/4	1.000
1/16	1.460	1	0.689
1/64	2.151	4	0.478
1/256	3.197	16	0.334

where $v_c(\mathbf{r}) = \delta E_c[n]/\delta n(\mathbf{r})$ is the correlation contribution to the Kohn-Sham potential. The method gives highly accurate energies for Hooke’s atom ($k = 1/4$) and for Helium when λ varies from 0 to 1. The error at $\lambda = 0$ is 0.3 mHartrees, and the estimated error for λ close to one less than 1 mHartree [17].

For each simulated scaling, we must assign an appropriate scale factor, but which true scaled density does the approximately scaled density mimic? The original paper discusses several possibilities. They all require knowing how a chosen component of the energy changes with uniform density scaling. We use the E_x method:

$$\lambda = 1/\gamma = E_x[n]/E_x[n']. \quad (10)$$

Since we use E_x to assign λ , the $U_x(\infty)$ contribution to $U_{xc}(\infty)$ necessarily scales properly for all values of λ , and so we show only $U_c(\mu = 0)$.

In this paper, we examine the adiabatic connection curve at large interaction strengths. This method only works for $\lambda > 1$ for systems that remain bound as the external potential is weakened. Even with this restriction, the method must ultimately fail as $\lambda \rightarrow \infty$. Specifically for Hooke’s atom, Cioslowski showed that at a certain critical strength for the external potential, $k_c = 0.0016$ ($\lambda_c = 4.138$), the density changes shape qualitatively [25]. Beyond this value, the simulated scaling might no longer be a good approximation to exact scaling. On the other hand, the method fails for He almost immediately as the two electron ion unbinds at nuclear charge, $Z = 0.9$.

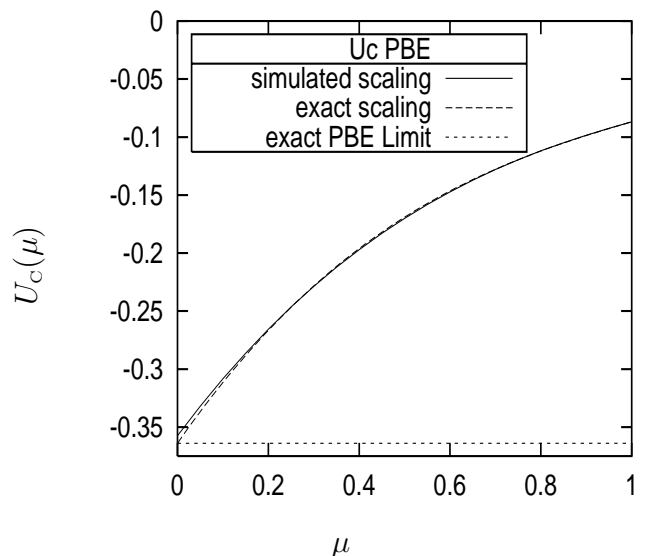


FIG. 2: PBE adiabatic connection curve for Hooke’s atom ($k = 1/4$): $U_c(\mu)$. The solid line is generated using simulated scaling of the density, and the dashed curve by exactly scaling the known functional. The exact PBE $U_c(\mu = 0)$ limit is shown (short dashes).

To test this procedure and to develop a rule for its

reliability, we apply the procedure in a case where we already know the correct answer, namely with an approximate functional. A generalized gradient approximation (GGA) mimics the complexity of the true functional better than, say, the local density approximation. Because of its first principle derivation and reliability, we use PBE here [26]. Since we have the analytic form for the PBE functional, we can scale the input density to generate the entire adiabatic curve, Fig. 2. The curve is shown as a function of $\mu = 1/\sqrt{\lambda}$ so that the region $\lambda \in 1, \infty$ can appear on a finite sized plot.

PBE results for certain key λ values are listed in Table IV. An explicit formula [15] for the PBE functional as $\mu \rightarrow 0$ is

$$U_{xc}^{PBE}(\infty)[n] = \int d^3r n(r)\epsilon_x(n) \left(F_x^{PBE}(s) + \frac{0.964}{1+y+y^2} \right) \quad (11)$$

where $y = 0.2263 s^2$, s is the reduced gradient, $\epsilon_x(n)$ is the exchange energy per particle of the uniform gas, and $F_x^{PBE}(s)$ is an exchange enhancement factor [26].

We need a criterion for how far along the adiabatic connection we can trust the simulated density scaling to mimic the exactly scaled density. Our criterion is to terminate the simulations at $\mu = \mu_c = 1/\sqrt{\lambda_c}$ where the density qualitatively changes shape [25]. Even at this point, the first order correction in Eq. (9) still improves upon the zeroth order simulation. This is a highly conservative estimate; it is likely that the curves are accurate to smaller μ 's.

To get a prediction for $U_c(\mu = 0)$, we must extrapolate the simulation to $\mu = 0$. This is done by fitting the simulated data to an n^{th} order polynomial and extrapolating this polynomial to $\mu = 0$. The third order polynomial connecting four sample points best reproduces the known $U_c^{PBE}(\infty)$. In Fig. 2, we show the exactly scaled PBE functional and the polynomial interpolation. We see that the simulated curve is almost on top of the exact curve. However, they do differ slightly in the $U_c(\mu = 0)$ values. For the simulated curve, $U_c(\mu = 0) = -0.357$, and the scaled result is -0.363 from Eq. (11), a 6 mHartree error.

IV. EXTRAPOLATING TO THE INFINITE INTERACTION STRENGTH LIMIT

The simulated adiabatic connection curve for Hooke's atom $k = 1/4$ in Fig. (3) approaches the SCE $U_c(\mu = 0)$ limit. As in section III for the PBE functional, we reproduce the entire curve by fitting the simulated points to a third order polynomial. Since the simulated scaling method is only reliable between $\mu_c = 1/2$ and 1, we must extrapolate the curve over the domain $\mu = 0$ to $1/2$ by a polynomial. The extrapolated prediction for $U_c(\mu = 0)$, -0.206 , is 22 mHartrees from the strictly correlated electron prediction, -0.228 . We do not expect as good agreement because the true E_c functional is more complicated

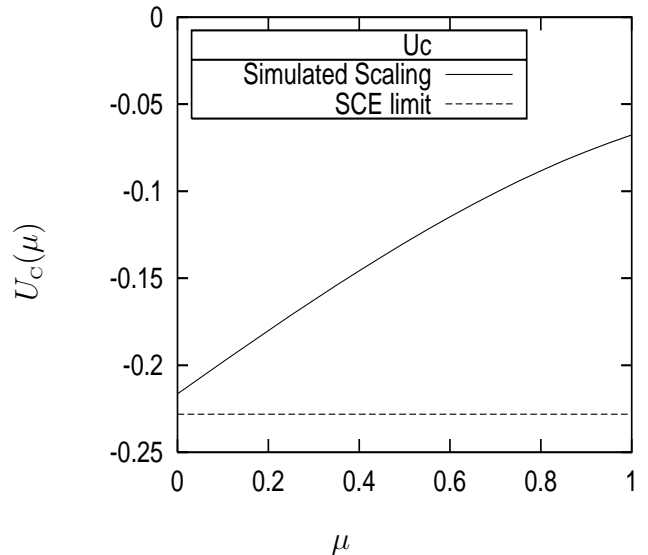


FIG. 3: The adiabatic connection curve for Hooke's atom ($k = 1/4$): $U_c(\mu)$. The solid line is the simulated curve. The SCE limit is shown as a dashed line.

than a GGA, and we regard the result as consistent with the SCE hypothesis.

V. SIMULATING THE ENTIRE ADIABATIC CONNECTION CURVE

In section IV, we used an extrapolation scheme to complete the adiabatic curve. Here, we combine the simulated part with the SCE electron limit to produce a highly accurate adiabatic connection curve for all coupling strengths. From this curve, we calculate the first terms in Taylor expansions about both $\lambda = 0$ and 1, and $\mu = 0$ and 1. Using these new results, we assess the accuracy of the Interaction Strength Interpolation (ISI) with accurate inputs.

TABLE II: Higher derivatives of $U_c(\mu)$ with respect to μ for Hooke's atom ($k = 1/4$).

μ	$U_c(\mu)$	$U_c'(\mu)$	$U_c''(\mu)$
0	-0.228	0.235	-0.156
1	-0.068	0.088	0.221

TABLE III: Higher derivatives of $U_c(\lambda)$ with respect to λ for Hooke's atom ($k = 1/4$).

λ	$U_c(\lambda)$	$U_c'(\lambda)$	$U_c''(\lambda)$	$U_c^{(3)}(\lambda)$	$U_c^{(4)}(\lambda)$
0	0.0000	-0.101	0.095	-0.107	0.124
1	-0.0677	-0.044	0.032	-0.032	0.039

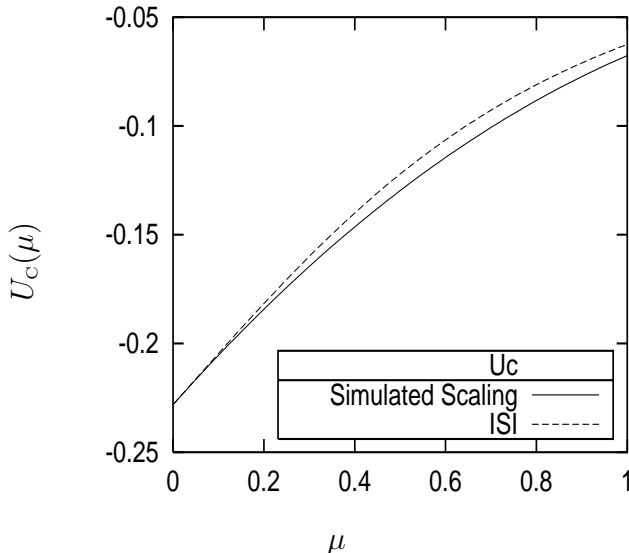


FIG. 4: Simulated adiabatic connection curve for Hooke's atom ($k=1/4$): $U_C(\mu)$. The solid line is the simulated curve with the SCE $U_C(\mu = 0)$. The dashed curve is the ISI using exact inputs.

TABLE IV: Accurate results for Hooke's atom with $k = 1/4$ evaluated on the exact densities.

	E_x	$2E_C^{GL2}$	E_C	$U_C(\mu = 1)$	$U_C(\mu = 0)$	$U'_C(\mu = 0)$
PBE	-0.493	-0.168	-0.051	-0.087	-0.363	0.561
Exact	-0.515	-0.101	-0.039	-0.068	-0.228	0.235

The $\mu < 1$ simulated adiabatic connection curve is shown in Fig. 4. The curve was generated by fitting the simulated data points from $\mu = 0.5$ to 1 and including the SCE $U_C(\mu = 0)$ in the point set. We used a third order polynomial, the order that best reproduced the adiabatic curve for the PBE functional in section III. This curve should be an excellent approximation to the exact curve. From the plot, we see that the derivative $dU_C(\mu)/d\mu$ is positive everywhere along the adiabatic curve. This implies that $dU_C(\lambda)/d\lambda$ is negative, and the adiabatic curve is convex. All calculated $U_C(\lambda)$ curves for $0 \leq \lambda \leq 1$ have $dU_C(\lambda)/d\lambda < 0$, but the inequality has never been generally proven. Our result extends this observation to $\lambda \geq 1$ for this system.

Derivatives of $U_C(\mu)$ are obtained from the coefficients in the polynomial extrapolation. Two higher derivatives of $U_C(\mu)$ with respect to μ are shown in table II. Seidl's model for $U'_C(\mu = 0) = 0.281$ [13] does not agree with the accurate $U'_C(\mu = 0)$. This indicates that the missing contributions to the SCE $U'_C(\mu = 0)$ mentioned by Seidl are, at least for this system, not negligible.

Several higher derivatives of $U_C(\lambda)$ with respect to λ are listed in table III. Here, we need not restrict ourselves to a third order polynomial interpolation because we have

TABLE V: Interaction Strength Interpolation Results for Hooke's atom with $k = 1/4$. *Accurate* and *model* refer to the value of $U'_C(\mu = 0)$. The accurate value is from our simulation and the model is from Seidel's model [13].

Method	$U'_C(\mu = 0)$	$U_C(\lambda = 1)$	Error	E_C	Error
ISI (accurate)	0.235	-0.063	8 %	-0.036	6 %
ISI (model)	0.281	-0.060	11 %	-0.035	9 %

a dense sampling of data points over the range $\lambda = 0$ to 4. The higher derivatives reported in terms of λ are expected to be highly accurate.

The interaction strength interpolation (ISI), as originally formulated [14], is an interpolation scheme for the entire adiabatic connection curve. It used exact values at $\lambda = 0$ and carefully chosen GGA values at $\mu = 0$. We now ask how well the ISI with accurate inputs compares to the simulated curve. The answer tells us how good the choice of curve in the ISI is. For the inputs to the ISI, we use the exact E_x and E_C^{GL2} which are derivable from the simulated curves in Ref. [17] and are given in Table IV. For $U_{xc}(\infty)$, we use the SCE prediction which judging from the results in section IV, we believe to be exact. For $U'_C(\mu = 0)$, we input two different values: the accurate simulated value and Seidel's prediction. The results are shown in table V. The ISI interpolation does not perform exceptionally well with accurate inputs as already noticed in [11]. For example, the magnitude of $U_{xc}(1)$ is underestimated by 5 mHartrees. This is perhaps a result of the way the $U'_C(\mu = 0)$ limit is included in the interpolation equation. For this system, incorporating the accurate value for $U'_C(\mu = 0)$ in the ISI does *not* greatly improve its accuracy.

In Fig. 5, we see how the PBE and LDA adiabatic connection curves compare to the accurate curve. The PBE curve clearly crosses the accurate curve. Since $\lim_{\mu \rightarrow 0} U_{xc}^{LDA}(\mu) = 1.964 E_x^{LDA} = -0.866 < U_{xc}(\infty)$, the LDA curve must cross the accurate one at some larger interaction strength. Since both curves cross the exact curve at some $\lambda > 1$, the cancellation of errors between exchange and correlation in E_{xc}^λ will grow smaller beyond some critical interaction strength and become an addition of errors. It has been argued that because the exchange correlation on-top hole grows more local as the interaction strength increases [10, 27], local functionals for E_{xc}^λ would work better as λ increases. This is certainly true for our system in the range, $0 \leq \lambda \leq 1$; however, the adiabatic plots indicate that as λ grows, the energy depends on the density in an increasingly nonlocal way. The accuracy of the on-top hole is less relevant to the total energies in the strongly interacting region of the adiabatic connection curve.

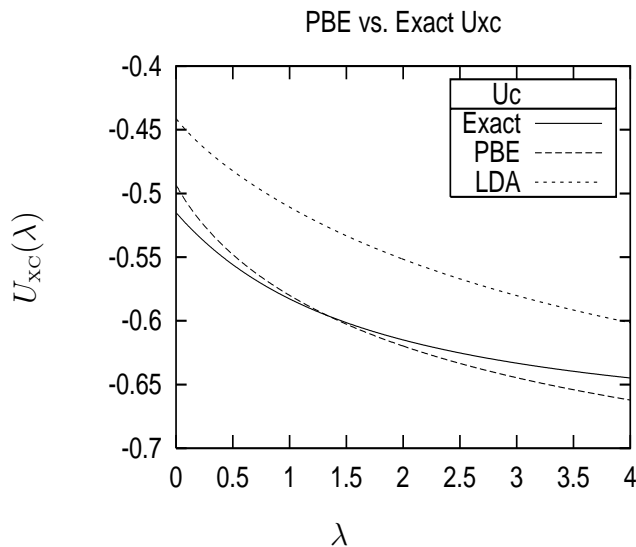


FIG. 5: Adiabatic connection curve for Hooke's Atom using various functionals: The exact curve is the solid line, the PBE is the long dashed line, and the local density approximation (LDA) is the short dashed line.

VI. CONCLUSION

In this work, we have extended the method of Ref. [17] to simulate the adiabatic connection curve to interaction strengths greater than the physical value for a simple model system. In doing so, we kept in mind that the method must fail at some μ_c as $\mu \rightarrow 0$ ($\mu = 1/\sqrt{\lambda}$) and performed an extrapolation to the strong interaction limit. This simulated curve agreed with the SCE hypothesis. To generate a highly accurate curve for $\mu = 0$ to 1, we included the SCE $U_c(\mu = 0)$ in the set of points and interpolated. Using this accurate adiabatic curve, we found higher derivatives at key coupling constants: $\lambda = 0, 1$, and ∞ . Finally, we compared some popular approximate functionals to the accurate curve. These results will be useful in the formal analysis of the adiabatic connection curve, the testing of approximate functionals, and the construction of new functionals in DFT.

VII. ACKNOWLEDGMENTS

We would like to thank John Perdew for discussions and Takeyce Whittingham for computationally checking $U_{xc}^{PBE}(\infty)$. This work supported by the National Science Foundation under grant number CHE-9875091.

REFERENCES

[1] *Nobel Lecture: Electronic structure of matter - wave functions and density functionals*, W. Kohn, Rev.

- Mod. Phys. **71**, 1253 (1999).
- [2] *Inhomogeneous electron gas*, P.Hohenberg & W. Kohn, Phys. Rev. **136**, B 864 (1964).
- [3] *Self-consistent equations including exchange and correlation effects*, W. Kohn & L.J. Sham, Phys. Rev. **140**, A 1133 (1965).
- [4] *The exchange-correlation energy of a metallic surface*, D.C. Langreth & J.P. Perdew, Solid State Commun. **17**, 1425 (1975).
- [5] *Exact Kohn-Sham scheme based on perturbation theory*, A. Görling & M. Levy, Phys. Rev. A **50**, 196 (1994).
- [6] *Toward reliable density functional methods without adjustable parameters: The PBE0 model*, C. Adamo & V. Barone, J. Chem. Phys. **110**, 6158 (1999).
- [7] *Density-functional thermo-chemistry. III. The role of exact exchange*, A.D. Becke, J. Chem. Phys. **98**, 5648 (1993).
- [8] *Mixing exact exchange with GGA: When to say when*, K. Burke, J.P. Perdew, & M. Ernzerhof, in *Electronic Density Functional Theory: Recent Progress and New Directions*, Eds. J.F. Dobson, G. Vignale, & M.P. Das (Plenum, NY, 1997), page 57.
- [9] *Rationale for mixing exact exchange with density functional approximations*, J.P. Perdew, M. Ernzerhof, & K. Burke, J. Chem. Phys. **105**, 9982 (1996).
- [10] *The adiabatic connection method: A non-empirical hybrid*, K. Burke, M. Ernzerhof, & J.P. Perdew, Chem. Phys. Lett. **265**, 115 (1997).
- [11] *Exploring the Adiabatic Connection Between Weak and Strong Interaction Limits in Density Functional Theory*, J. Perdew, S. Kurth, & M. Seidl, International Journal of Modern Physics D, Vol. **15**, 1672 (2001).
- [12] *Strictly correlated electrons in density functional theory*, M.Seidl, J. Perdew, & M. Levy, Phys. Rev. A **59**, 51 (1999).
- [13] *Strong-interaction limit of density-functional theory*, M.Seidl, Phys. Rev. A **60**, 4287 (1999).
- [14] *Simulation of All-Order Density-Functional Perturbation Theory, Using the Second Order and the Strong-Correlation Limit*, M.Seidl, J. Perdew, & S. Kurth, Phys. Rev. Lett. **84**, 5070 (2000).
- [15] *Density functionals for the strong interaction limit*, M.Seidl, J. Perdew, & S. Kurth, Phys. Rev. A **62**, 012502 (2000).
- [16] *Improving energies by using exact electron densities*, K. Burke, J.P. Perdew, and M. Levy, Phys. Rev. A **53**, R2915 (1996).
- [17] *Adiabatic connection from accurate wave-function calculations*, D. Frydel, W. Terilla, & K. Burke, J. Chem. Phys. **112**, 5292 (2000).
- [18] *Density functionals and dimensional renormalization for an exactly solvable model*, S. Kais, D.R. Herschbach, N.C. Handy, C.W. Murray, and G.J. Laming, J. Chem. Phys. **99**, 417 (1994).
- [19] *Energy spectra of two electrons in a harmonic quantum dot*, U. Merkt, J. Huser, & M. Wagner, Phys.

- Rev. B **43**, 7320 (1991).
- [20] *Correlation energies for two interacting electrons in a harmonic dot*, R. M. G. Garca-Casteln, W. S. Choe, & Y. C. Lee Phys. Rev. B **57**, 9792-9806 (1998)
- [21] *Two electrons in an external oscillator potential: Particular analytic solutions of a Coulomb correlation problem*, M. Taut, Phys. Rev. A **48**, 3561 (1993).
- [22] *Requirements for Correlation Energy Density Functionals from Coordinate Transformations*, A. Görling & M. Levy, Phys. Rev. A **45**, 1509 (1992).
- [23] *Digging into the exchange-correlation energy: The exchange-correlation hole*, K. Burke in *Electronic Density Functional Theory: Recent Progress and New Directions*, eds. J.F. Dobson, G. Vignale, & M.P. Das (Plenum, NY, 1997), page 19.
- [24] *Hellmann-Feynman, virial, and scaling requisites for the exact universal density functionals. Shape of the correlation potential and diamagnetic susceptibility for atoms*, M. Levy & J.P. Perdew, Phys. Rev. A **32**, 2010 (1985).
- [25] *The ground state of harmonium*, J. Cioslowski, K. Pernal, J. Chem. Phys. **113**, 8434 (2000).
- [26] *Generalized gradient approximation made simple*, J.P.Perdew, K.Burke, & M.Ernzerhof, Phys. Rev. Lett. **77**, 3865 (1996); **78**, 1396 (1997) (E).
- [27] *Why semilocal functionals work: Accuracy of the on-top pair density and importance of system averaging*, K. Burke, J. Perdew, & M. Ernzerhof, J. Chem. Phys. **109**, 3760 (1998).